10th World Congress on Structural and Multidisciplinary Optimization
May 19 -24, 2013, Orlando, Florida, USA

Experimental Optimization and Uncertainty Quantification of Flapping Wing of a Micro Air Vehicle

Anirban Chaudhuri[δ,]*, Raphael T. Haftka[δ], Peter Ifju[δ], Diane Villanueva[δ], Kelvin Chang[δ], Jason Rue[δ], Christopher Tyler[†], Tony Schmitz[†]

[δ]University of Florida, Gainesville, FL, USA
{a.chaudhuri@ufl.edu, haftka@ufl.edu, ifju@ufl.edu, dvillanu@gmail.com, kc3635@ufl.edu, gatorrue@ufl.edu}

[†]University of North Carolina at Charlotte, NC, USA
{ctyler6@uncc.edu, Tony.Schmitz@uncc.edu}

Abstract
Recently, there has been an increase in interest in flapping wing micro air vehicles as they are capable of hover and forward flight with high maneuverability. Flapping wing flight is difficult to simulate accurately as it is a much more complex phenomena than fixed wing or rotorcraft. Consequently the optimization of flapping wing based on simulation is challenging and, therefore, we have elected to optimize a wing experimentally. Specifically, we use experimental data to optimize the flapping wing structure for maximum thrust production in hover mode. The flapping wing has a quarter-ellipse planform made of a nylon membrane (Capran 1200 Matte) with unidirectional carbon fiber battens making unique structural patterns. Experimental optimization is hampered by noisy data, which for our wing is due to manufacturing variability and testing/measurement errors. These uncertainties need to be reduced to an acceptable level, and this requires us to quantify them. Multiple wings with identical nominal geometry are constructed to quantify manufacturing uncertainty and multiple tests on the same wing are conducted to quantify testing uncertainty. Then improvements in manufacturing and testing procedure are undertaken in order to reduce the noise. Another challenge is to reduce the number of experiments performed as it is time consuming and expensive to manufacture and test wings. This is done by using surrogates or meta-models to approximate the response (in this case, thrust) of the wing based on an initial design of experiments. In order to take into account the uncertainty or noise in the response we use gaussian process surrogates with noise and 2nd order polynomial response surface. Then a surrogate-based optimization algorithm called Efficient Global Optimization is used with different sampling criteria and multiple surrogates. This enables us to select multiple points per optimization cycle which is especially useful in this case as it is more time efficient to manufacture multiple wings at once. In this study, we have selected aspect ratio, leading edge stiffness and batten configurations as the design variables based on prior experience.

Keywords: Experimental optimization, Uncertainty quantification, Surrogate based optimization, Flapping wing MAV, Reasonable design space.

1. Introduction

Flapping wing micro air vehicles (FWMAVs) are garnering interest because of its high maneuverability with the ability to hover as well as forward flight. Flapping wings were also found to produce more lift especially for smaller size micro air vehicles (MAVs) [1], [2]. Numerous studies have been performed on the mechanics and aerodynamics of flapping wings. A widespread approach in development of FWMAV has been to mimic natural species [3]-[7] which has led to in-depth research in the study of dragonflies [8]-[12], Manduca sexta [13]-[17], hummingbirds [3], [18] and other flying creatures.

Previous works dealt with simulating the flapping wing kinematics [2], [19] and the effect of wing geometries [20]. There are also some studies on the optimization of flapping wing based on simulation models [20], [22]. However, it is difficult to calculate accurately the aerodynamic loads generated by a flapping wing, as it requires three dimensional transient CFD at low Reynolds numbers. Therefore, experimental optimization may be a reasonable alternative. In this work we undertake to find the optimum configuration of a flapping wing structure to maximize thrust. The collection of thrust data for flapping wing structure is done using an experimental set-up [21]. Experimental optimization of similar type was also undertaken by Viana et al. in optimization of a paper helicopter design [23].

A major challenge dealt with here is the analysis of data for quantifying multiple uncertainties due manufacturing and testing. Reliable uncertainty quantification allows us to decide on measures needed to reduce the uncertainty with an answer to whether to target the testing or the manufacturing process or both. Quantifying

*** Corresponding Author**

the uncertainty also leads to more effective optimization.

An additional challenge we face in experimental optimization is to reduce the number of experiments performed as it is time consuming and expensive to manufacture and test wings. This is done by using surrogates to approximate the response (in this case, thrust) of the wing based on an initial design of experiments. The surrogates used in this work are Gaussian Process (GP) with noise and 2nd order Polynomial Response Surface (PRS) which can handle noise in experimental data. A surrogate-based Efficient Global Optimization (EGO) [24]-[26] algorithm is employed with different sampling criteria and two surrogates. This enables us to select multiple points per optimization cycle which is advantageous as it is more time efficient to manufacture multiple wings at once. The human effort associated with manufacturing and performing the experiment dictates that we test multiple designs per cycle. It also serves as an insurance against some failed designs. For this work we have selected: (a) aspect ratio; (b) leading edge stiffness; and (c) batten configuration, as the design variables based on prior experience.

The remainder of the paper is arranged as follows. Section 2 provides details concerning the experimental set-up and manufacturing process. Section 3 explains and compares some methods of uncertainty quantification for limited data. Section 4 provides the necessary information about selection of points by EGO. Section 5 presents results and discussion. Concluding remarks and future work for this research are included in Section 7.

2. Manufacturing and Experimental Set-up

The manufacturing of the wing should be as repeatable as possible which led to the use of CNC to mill a Delrin (Acetal Resin) frame [21]. A pre-cured commercially available carbon fiber circular rod is attached in a trough on the leading edge to increase its stiffness while keeping the weight of the wing to a minimum. To establish a strong bond between the frame and rod, rubber toughened cyanoacrylate glue was applied. The completed frame is then glued to a nylon membrane, 14 micron thick sheet created by Honeywell, called Capran 1200 Matte.

The flapping mechanism secures the wings at a triangular plate in the corner where root and leading edge meet. A DC rotary motor (EC16 Maxon) drives the mechanism, while an EPOS 24/1 controller is used to dictate the flapping frequency with the help of a built-in encoder at the rear of the motor. The wings are flapped at 30 Hz with a flapping angle of ± 48°. The mechanism is mounted on a 6 axis force and torque sensor (Nano17 from ATI automation) which is read by a 16-bit DAQ device (NI USB-6251). Both the controller and sensor are managed with separate LabVIEW virtual instruments. A photograph of the set-up can be seen in Figure 1.

This experimental and manufacturing set-up evolved to bring the manufacturing and testing uncertainties under an acceptable level (<5%) for starting the optimization process. The method of quantification of these uncertainties is described in the next section.

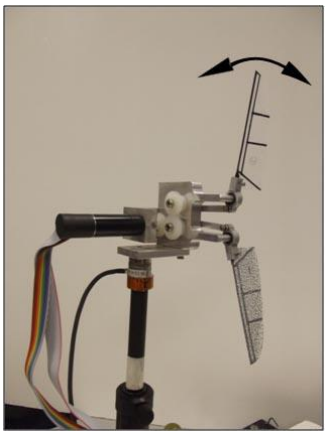

Figure 1. Flapping wing experimental set-up

3. Uncertainty Quantification of manufacturing and testing uncertainties

Two major sources of uncertainty are present in this experimental process: manufacturing and testing. Both uncertainties need to be quantified based on limited data. The uncertainty in the manufacturing process is mostly due to the tolerance of the machine as well as human error, while the testing uncertainty is present due to the sensor and testing conditions. Multiple replicates of wings with identical nominal geometry are constructed to quantify manufacturing uncertainty, and multiple tests on the same wing are conducted to quantify testing uncertainty. It is assumed that the uncertainties are defined by normal distribution.

Then we looked at the linear correlation coefficient between thrust data and individual standard deviations or coefficient of variations (CV) of both uncertainties. For testing uncertainty, we used 33 flapping wings (detailed description in Section 5.1) with 10 measurements for each of them. For manufacturing uncertainty, we used 4 replicates of 5 of these wings. For both testing and manufacturing uncertainties the correlation coefficient between individual standard deviations and thrust was higher, as shown in Table 1, indicating that the error scales with the

magnitude of thrust. Therefore, the decision was made to use normal distributions with fixed coefficient of variation for both testing (CV_{test}) and manufacturing (CV_{mfg}) uncertainties.

Table 1. Correlation between thrust and standard deviations or coefficient of variation of flapping wing data

Type of Uncertainty	**Correlation Coefficient**	
	Standard deviations and thrust	**Coefficient of variations and thrust**
Testing Uncertainty	**0.52**	-0.20
Manufacturing Uncertainty	**0.94**	0.79

3.1. Estimate using unbiased root mean square approach

The root mean square approach for individual coefficient of variations [28], [29] instead of arithmetic mean is used to quantify the testing and manufacturing uncertainties. This is implemented by getting the coefficient of variations of set of data for each design, squaring them, taking the mean, and then taking the square root of the mean.

3.1.1. Correcting Bias

The commonly used Bessel correction rectifies the bias in the estimate of sample variance for *n* samples as,

$$(\sigma^2)_{unbiased} = \frac{n}{n-1}(\sigma^2)_{biased} \tag{1}$$

However, for small sample sizes, the process of taking the square root of the variance to obtain the standard deviation introduces a bias in the standard deviation estimate [30]. The expected bias in general is a function of a process distribution which in this case is assumed to be normal. Therefore, a simple bias correction can be done for normal distributions using a correction factor ($c_4(n)$) that depends on the sample size[30]. Equation (2) is used to get an unbiased estimate of the standard deviation, $s_{unbiased}$. This unbiased estimate of standard deviation can now be used to compute the unbiased coefficient of variation.

$$s_{unbiased} = \frac{\sqrt{(\sigma^2)_{unbiased}}}{c_4(n)} \tag{2}$$

Table 2. List of correction factors for different sample sizes [30]

Sample size	**Correction Factor, $c_4(n)$**
4	0.9213
10	0.9727

3.1.2. Quantifying testing uncertainty

To quantify testing uncertainty, unbiased coefficient of variation (CVt_i) of 10 measurements of each wing is found. Then the root mean squared approach is used with the unbiased CVt_i to find CV_{test} as shown in Equation (3) . *d* is the total number of designs for which testing data is available.

$$CV_{test} = \sqrt{\frac{\sum_{i}^{d}\left(\frac{CVt_i}{c_4(n)}\right)^2}{d}} \tag{3}$$

3.1.3. Quantifying manufacturing uncertainty

To compute CV_{mfg}, the means of 10 measurements for each replicated design was found (sampled manufactured means). Then the unbiased coefficient of variation in the manufactured means (CVm_j) for each design with root mean squared approach is used to quantify CV_{mfg} as given by Equation (4). Implementation of the method can be seen in Figure 2. *N* is the number of designs for which replicates are available.

Design 1:
Replicate 1: 10 measurements – Manufactured Mean 1
Replicate 2: 10 measurements – Manufactured Mean 2
Replicate 3: 10 measurements – Manufactured Mean 3
Replicate 4: 10 measurements – Manufactured Mean 4
→ CV in manufactured means for 1st design (CVm_1)

Design 2:
Replicate 1: 10 measurements – Manufactured Mean 1
Replicate 2: 10 measurements – Manufactured Mean 2
Replicate 3: 10 measurements – Manufactured Mean 3
Replicate 4: 10 measurements – Manufactured Mean 4
→ CV in manufactured means for 2nd design (CVm_2)

---- ***N* designs that are replicated.**

Figure 2. Process of quantifying manufactured uncertainty

$$CV_{mfg} = \sqrt{\frac{\sum_{j}^{N}\left(\frac{CVm_j}{c_4(n)}\right)^2}{N}} \quad (4)$$

3.2. Results for a test case

In order to analyze the accuracy of the method, an artificial test case with 10 different designs is created with true mean thrust values, manufacturing and testing uncertainties, and number of replications as shown in Table 3. First CV_{mfg} is used with respective true mean thrusts to create manufactured means for each of the replicated designs indicated. In case of designs 6-10, there is just 1 design which is generated using CV_{mfg} and true mean thrust to create one manufactured mean. Then CV_{test} is used to generate raw data comprising of 10 measurements for each case of manufactured mean. There are 4 replicates of designs 1-5 and 1 design for designs 6-10 (5*4+5*1 = 25 cases in total). All 25 cases are used for quantifying testing uncertainty, and replicates of designs 1-5 are used to quantify manufacturing uncertainty. In order to reduce the randomness in comparison, the process was repeated 10 times.

Table 3. Parameters for creating artificial test case

Design Number	**True mean thrust (g)**	**Number of replications of identical nominal geometry**	**Coefficient of Variation**	
			True Testing uncertainty, CV_{test}	**True Manufacturing uncertainty, CV_{mfg}**
1.	3.5	4	3.5%	3%
2.	5.0			
3.	4.2			
4.	6.5			
5.	8.0			
6.	9.5	1		
7.	2.8			
8.	5.5			
9.	3.7			
10.	8.5			

The correction factors ($c_4(n)$) for testing uncertainty for a sample size $n=10$ (10 measurements for each design), and for manufacturing uncertainty for a sample size $n= 4$ (number of replicates of each design) are taken from Table 2.

The results obtained as a mean of 10 different test cases generated using the parameters in Table 3 are given in Table 4. The estimate using unbiased root mean square approach is compared to the case of just taking arithmetic mean of individual unbiased coefficient of variations. It can be seen that the estimates using unbiased root mean square approach are conservative but very close to the true values as compared to the unconservative estimate using the arithmetic mean.

Table 4. Estimated manufacturing and testing uncertainty presented as mean of 10 test cases

Method	**Testing Uncertainty, CV_{test}**		**Manufacturing Uncertainty, CV_{mfg}**	
	Mean	**Standard deviation**	**Mean**	**Standard deviation**
Estimate using unbiased root mean square approach	3.56%	0.2	3.15%	0.4
Arithmetic mean of unbiased coefficient of variations	3.48%	0.2	2.96%	0.5
True values	3.5%	--	3%	--

4. Background: Efficient Global Optimization

A brief description of the Efficient Global Optimization (EGO) algorithm developed by Jones et al.[24], [25] is provided followed by a description of multi-point selection per optimization cycle.

4.1. EGO

Firstly an initial set of data points is fitted with a Kriging model as a realization of a Gaussian Process with a mean of $\hat{y}(x)$ and a standard deviation of $s(x)$. Then each cycle consists of selecting additional points based on maximizing the expected improvement (EI) or probability of targeted Improvement (PI) and refitting the surrogate. Figure 3 illustrates the EGO algorithm with maximizing PI for a given target using a Kriging surrogate for a one dimensional function without noise at the data points. After adding the new point to the existing data set,

the Kriging model is updated and the process continues until a stopping criterion is met (usually number of cycles). Commonly Kriging is used for EGO, but any surrogate that provides an uncertainty estimate can be used. In this work Gaussian Process (GP) with noise and 2nd order Polynomial Response Surface (PRS) are used as the surrogates as they can account for noise in the experimental data. For simplicity, we fit the mean of the collected data for each design. EGO and its sampling criteria are explained based on a minimization problem. Therefore here we minimize the negative of thrust values which is equivalent to maximizing the thrust.

4.2. Probability of targeted Improvement (PI)

The probability of improving the objective beyond a target, y_{Target}, at a point x is given by Equation (5) [25], [26], [27].

$$\mathrm{P}\,I(x) = \Phi\left(\frac{y_{T\,\mathrm{arg}\,et} - \hat{y}(x)}{s(x)}\right) \tag{5}$$

where, Φ (.) is the cumulative density function of a normal distribution, $\hat{y}(x)$ is the surrogate prediction, $s(x)$ is the prediction standard deviation (square root of the prediction variance). EGO-PI easily provides multiple new design points per optimization cycle [26], [27] which is especially useful in this case as it is more time efficient to manufacture multiple wings at once.

4.3. Expected Improvement (EI)

Another way of selecting points is to maximize the expected improvement [24], [25] upon the Present Best Solution (PBS), y_{PBS}. In this case y_{PBS} is given by the lowest mean of the collected data. The Expected Improvement (EI) is given by Equation (6).

$$EI(x) = (y_{PBS} - \hat{y}(x))\Phi\left(\frac{y_{PBS} - \hat{y}(x)}{s(x)}\right) + s(x)\phi\left(\frac{y_{PBS} - \hat{y}(x)}{s(x)}\right) \tag{6}$$

where, $\phi(.)$ is the probability density function of a normal distribution.

4.4. Selecting multiple points per cycle

As it is more time efficient to manufacture and test multiple wings at a time, 22 new designs were generated using EGO and two different surrogates, namely, Gaussian Process (GP) and Polynomial response surface of 2nd order (PRS), along with different infill criteria (PI and EI) as shown in Table 5.

Table 5. 22 new points found using EGO with different surrogates and different infill criteria

Type of Surrogate	Infill Criteria for EGO	Number of points added per EGO cycle
Gaussian Process with noise	**PI with 10% initial Target of Improvement**	**5**
	PI with 25% initial Target of Improvement	**5**
	EI	**1**
2nd order Polynomial Response Surface	**PI with 10% initial Target of Improvement**	**5**
	PI with 25% initial Target of Improvement	**5**
	EI	**1**

Out of 22, the unique designs are found and then, a constraint on the distance between new designs and already present designs was introduced to exclude any design that falls within an exclusion radius given by,

$$eps = \sqrt[3]{\frac{1}{\frac{4\pi}{3} d_{budget}}} \tag{7}$$

where, $d_{budget} = 100$ in this case and represents the number of designs we expect to test.

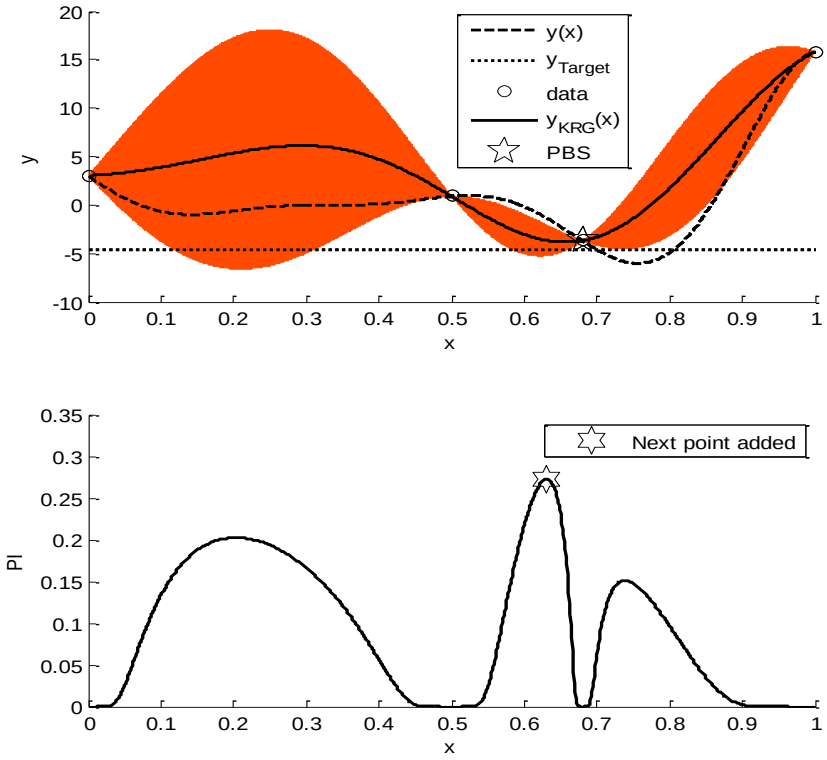

Figure 3.One cycle of EGO using PI for a one dimensional test function [$y(x) = (6x-2)^2 sin(12x-4)$] with initial data set as $x = [0\ 0.5\ 0.68\ 1]^T$. The uncertainty (amplified amplitude of $2*s(x)$) associated with the kriging is plotted in orange. The target, y_{Target} is set below PBS.

5. Results and Discussion

In this work we optimize with a small number of variables, 3, in order to understand the issues faced while doing experimental optimization. The constant features of the wing geometry include a batten at the root at 90° from the horizontal (as shown in orange in Figure 4) and one other batten starting at the intersection of root and leading edge. The additional batten can be set at different angles. The three design variables which define the wing structure, were selected based on prior experience and are described in Table 6. The initial design of experiment (DOE) of 20 design points was created using Latin hypercube sampling [31] while maximizing the minimum distance between the points.

$$\text{Length of carbon rod} = (\text{Stiffness percentage}) * (\text{Length of leading edge}) \quad (8)$$

Table 6. Design variables

Design Variable	Description	Lower Bound	Upper Bound
Aspect Ratio Number	Manufacturing constraints force us to restrict aspect ratio to 6 different choices between 3 and 14. A particular number is assigned to each of the aspect ratios and called aspect ratio number (Table 7) which makes it easier to deal with the discrete variable in optimization. All wings have same planform area as normalization criteria.	**1**	**6**
Stiffness Percentage	Stiffness of leading edge in terms of the length of the cylindrical rod added to the plastic wing. This is determined as a percentage of the leading edge length. This is shown by the green solid line in Figure 4. The length of the carbon rod to be glued is given by Equation (8).	**25 %**	**100 %**
Angle of Batten	This defines the angle of the batten starting at the intersection of root and leading edge. The angle is measured in a clockwise direction from the horizontal (shown by blue dashed line in Figure 4). This is a discrete variable with only integers possible owing to our manufacturing precision.	**1°**	**80°**

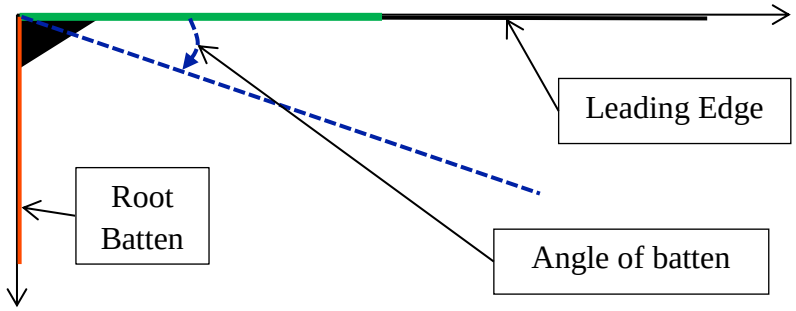

Figure 4. Design variables: Angle of batten (blue dashed line) and stiffness percentage of the leading edge (green)

Table 7. Definition of wing geometries corresponding to 6 choices of aspect ratio (all wings have similar area with some rounding-off error)

Aspect Ratio Number	**Leading Edge length, $\frac{b}{2}$ (mm)**	**Root length (mm)**	**Area, S**	**Aspect Ratio, $\frac{b^2}{S}$**
1	47	39.89	2945	3.0
2	55	34.09	2945	4.1
3	75	25.00	2945	7.6
4	82	22.87	2946	9.1
5	91	20.60	2945	11.3
6	101	18.56	2945	13.9

5.1. Revised Design Space

From the results of the initial 20 designs it became clear that some regions of the design space had small thrust values or unstable designs which failed during testing. One of the designs failed due to manufacturing issues. The major contributors in failed designs were found to be the stiffness percentage and the angle of batten from an initial inspection of the data. The thrust values also for lower values of both these variables showed poor performance as shown in Figure 5. So it was decided to change the range of the variables.

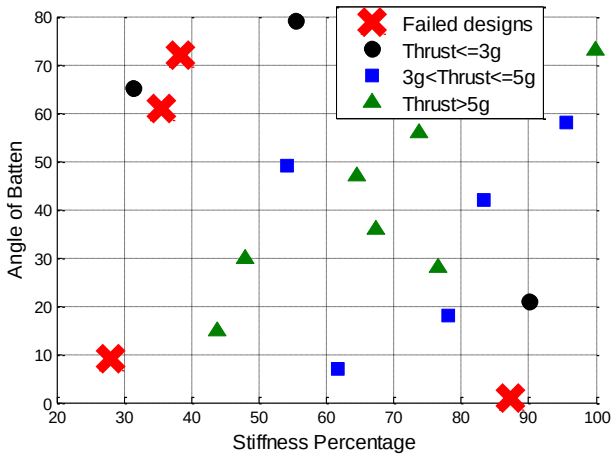

Figure 5. Results for the initial DOE showing different levels of thrust and failed designs w.r.t. stiffness percentage and angle of batten

In order to decide on the reduction of the design space, a Gaussian Process (GP) surrogate was fitted to data with the quantified testing and manufacturing noise. All the data available from the first 20 designs were used except 2, whose testing was inconclusive. The surrogate has high error percentage (root mean squared cross validation error [32] ~ 27%). However, we considered it good enough to identify regions with very bad designs. Figure 6 summarizes the predictions by showing slices of design space with respect to stiffness percentage and angle of batten.

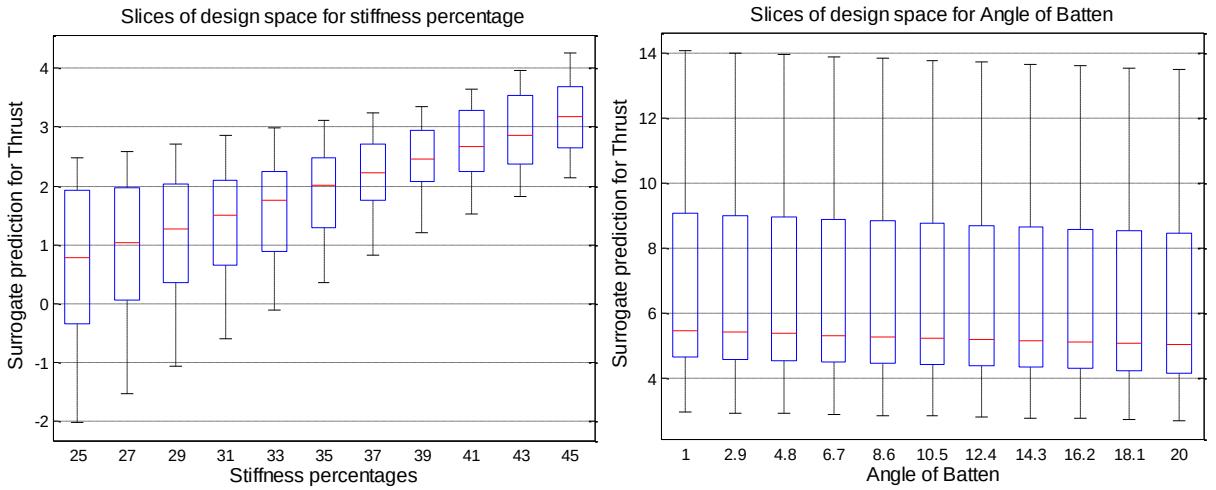

(a) **(b)**

Figure 6. Surrogate predictions using for slices of design space to show thrust variation according to (a) Stiffness percentage, (b) Angle of batten

Figure 6(a) indicates that a stiffness percentage below 40% produces thrusts of less than 3g. Therefore, the lower bound of stiffness percentage was raised to 40%. Figure 6(b) did not provide clear indication on the lower bound of the batten angle, so the bound was raised from 1° to 10° as at lower angles the flapping motion was unstable owing to high flexibility and there was substantial damage to the wing.

It was also noticed that the highest values of thrust were obtained at the higher aspect ratios. So two higher aspect ratios were added as shown in Table 8. But after testing 3 designs for aspect ratio number of 7 and 8 each it was found that those designs failed either due to unstable structure or very high power consumption. So the range of aspect ratio was kept the same as before. The revised range for design space is given in Table 9. A new DOE of 20 design points was generated in the revised design space using Latin hypercube sampling. 13 designs from the initial DOE also fell in the revised range and that provided a total of 33 designs for analysis.

Table 8. Details for Aspect Ratio Numbers 7 and 8

Aspect Ratio Number	**Leading Edge length, $\frac{b}{2}$ (mm)**	**Root length (mm)**	**Area, S**	**Aspect Ratio, $\frac{b^2}{S}$**
7	105	17.9	2946	14.9
8	115	16.3	2944	18

Table 9. Revised range for design space

Design Variable	**Lower Bound**	**Upper Bound**
Aspect Ratio Number	**1**	**6**
Stiffness Percentage	**40 %**	**100 %**
Angle of Batten	**10°**	**80°**

5.2. Uncertainty quantification for FWMAV

The uncertainties associated with the FWMAV data are shown in Table 10. The 33 designs from the initial and revised DOE are measured 10 times each to account for testing uncertainty. 5 of those designs with noticeably different thrust productions and different geometries are replicated 4 times to account for manufacturing uncertainty. Table 10 shows that the estimate using unbiased root mean square approach is more conservative. It can be seen that the testing and manufacturing uncertainty are 3.55% and 3.15% respectively which are acceptable for starting optimization (<5%).

Table 10. Estimated manufacturing and testing uncertainty for FWMAV data

Method	**Testing Uncertainty, CV_{test}**	**Manufacturing Uncertainty, CV_{mfg}**
Estimate using unbiased root mean square approach	3.55%	3.15%
Arithmetic mean of unbiased coefficient of variations	2.14%	3.04%

5.3. Experimental optimization results

For fitting surrogates, 33 data points are used. The root mean squared cross validation errors are 7.7% and 9.1% for GP and PRS, respectively. Number of designs (out of 33) with thrust>5g are 18, 3g<thrust≤5g are 11 and thrust≤3g are 4. The highest mean thrust in this data set is 11.1g.

22 new potentially optimum designs are generated using EGO as described in Section 4.4. There are 15 out of 22 distinct designs. After introducing the constraint on the minimum distance between the designs we are left with 6 new designs, shown in Table 11. The table also shows the mean thrust values of 10 measurements at 30Hz when these designs were tested. Wing 47 suffered structural damage during experimentation and testing of Wing 50 was not possible due to its high power consumption. Wings 49 and 51 improved our previous best solution of 11.1g by around 7%. The results also indicate that the optimum is pushing the upper limit boundary of both aspect ratio number and stiffness percentage.

Table 11. New designs left after implementing the distance constraint.

Wing No.	Aspect Ratio Number	Stiffness percentage	Angle of Batten (degrees)	Experimental mean thrust value (g)
47.	6	91.7241	10	--
49.	6	95.8621	20	11.8
50.	6	100.0000	10	--
51.	6	100.0000	29	11.9
52.	6	100.0000	40	10.4
53.	6	100.0000	50	10.6

6. Conclusions and Future Work

We performed experimental optimization of flapping wing structure for an MAV along with a technique to quantify multiple sources of uncertainty. In order to deal with the expensive nature of the experiment surrogate based optimization technique of EGO was utilized. A summary of our work is given below.

- We presented a method to quantify multiple sources of uncertainty from testing and manufacturing from limited samples using an unbiased root mean square approach for coefficient of variation. Application of the method to a few test cases showed that it is a very good and slightly conservative predictor.
- The initial design space was revised on the basis of an initial surrogate.
- EGO was used with multiple surrogates (GP and PRS) with different infill sampling criteria in order to generate multiple designs (22) per optimization cycle and a distance constraint based on available budget was applied on that to get new designs. First cycle of optimization was able to improve the initial best design by ~7%.

The process of manufacturing and testing a set of wings took 2-3 weeks. So this entire process took us around 4 months. A few more optimization cycles will be undertaken in the future to see if other interesting areas of design space crop up. After identifying the promising area with initial cycles of optimization Aspect Ratio will be made a continuous variable in that region to find the optimum design. Further improvements to the manufacturing and testing procedures will also help in development of the flapping wing structure.

Acknowledgements

This work was supported by Air Force Office of Scientific Research (AFOSR) grant FA9550-11-1-0066 from Dr. David Stargel, Grant Monitor.

References

[1] Ellington C.P., Berg C. van den, Willmott, A.P. and Thomas, A.L.R., Leading-edge vortices in insect flight, *Nature*, Vol. 384, Issue 19/26, 626-630, 1996.

[2] Dickinson M.H., Lehmann F.-O. and Sane S.P., Wing Rotation and the Aerodynamic Basis of Insect Flight, *Science*, 284 (5422), 1954 – 1960, 1999.

[3] Keenmon M., Klingebiel K., Won H. and Andriukov A., Development of the Nano Hummingbird: A Tailless Flapping Wing Micro Air Vehicle, *50th AIAA Aerospace Sciences Meeting including the New Horizons Forum and Aerospace Exposition*, Nashville, Tennessee, 9-12 January 2012 (10.2514/6.2012-588).

[4] de Croon G.C.H.E., de Clerq K.M.E., Ruijsink R., Remes B. and de Wagter C., Design, aerodynamics, and vision-based control of the DelFly, *International Journal of Micro Air Vehicles*, 1 (2), 71-97, 2009.

[5] Pornsin-Sirirak T.N., Tai Y.C., Ho C.H. and Keennon M., Microbat-A palm-sized electrically powered omithopter, *NASA/JPL Workshop on Biomorphic Robotics*, Pasadena, USA, 2001.

[6] Kawamura Y., Souda S., Nishimoto S. and Ellington C.P., Clapping-wing micro air vehicle of insect size, *Bio-mechanisms of swimming and flying*, Kato N and Kamimura S (eds), Springer Verlag, 319–330, 2008.

[7] Lentink D., Jongerius S.R. and Bradshaw N.L., The scalable design of flapping micro air vehicles Inspired by insect flight, *Flying Insects and Robots*, Floreano D, Zufferey JC, Srinivasan MV and Ellington CP (eds), Springer-Verlag, 185-205, 2009.

[8] Jongerius S.R. and Lentink, D., Structural Analysis of a Dragonfly Wing, *Experimental Mechanics*, 50 (9), 1323–1334, 2010.

[9] Tamai M., Wang Z., Rajagopalan G., Hui H. and He G., Aerodynamic performance of a corrugated dragonfly airfoil compared with smooth airfoils at low Reynolds numbers, *Proceedings of the 45th AIAA Aerospace Sciences Meeting and Exhibit*, Reno, Nevada, 8-11 January 2007 (10.2514/6.2007-483).
[10] Kesel A.B., Philippi U. and Nachtigall W., Biomechanical aspects of the insect wing: an analysis using the finite element method, *Computers in Biology and Medicine*, 28 (4), 423-437, 1998.
[11] Azuma A., Azuma S., Watanabe I. and Furuta T., Flight mechanics of a dragonfly, *Journal of experimental biology*, 116 (1), 79-107, 1985.
[12] Ren H., Wang X., Li X. and Chen Y., Effects of Dragonfly Wing Structure on the Dynamic Performances, *Journal of Bionic Engineering*, 10 (1), 28-38, 2013.
[13] Combes S.A., Daniel T.L., Into thin air: contributions of aerodynamic and inertial-elastic forces to wing bending in the hawkmoth Manduca sexta, *The Journal of Experimental Biology*, 206, 2999–3006, 2003.
[14] Combes S.A. and Daniel T.L., Flexural stiffness in insect wings II. Spatial distribution and dynamic wing bending, *The Journal of Experimental Biology*, 206, 2989-2997, 2003.
[15] Willmott A. P. and Ellington C. P., The mechanics of flight in the hawkmoth Manduca sexta. I. Kinematics of hovering and forward flight. *The Journal of Experimental Biology*, 200, 2705-2722, 1997.
[16] Wootton R.J., Herbert R.C., Young P.G. and Evans K.E., Approaches to the structural modeling of insect wings, *Philosophical Transactions of Royal Society B*, 358, 1577–1587, 2003.
[17] O'Hara R.P. and Palazotto A.N., The morphological characterization of the forewing of the Manduca sexta species for the application of biomimetic flapping wing micro air vehicles, *Bioinspiration & biomimetics*, 7 (4), 2012 (046011).
[18] Hedrick T.L., Tobalske B.W., Ros I.G., Warrick D.R. and Biewener A.A., Morphological and kinematic basis of the hummingbird flight stroke: scaling of flight muscle transmission ratio, *Proceedings of The Royal Society B (Biological sciences)*, 279 (1735), 1986-1992, 2012.
[19] Ansari S.A., Zbikowski R. and Knowles K., Insectlike Flapping Wings in the Hover Part 1: Effect of Wing Kinematics, *Journal of Aircraft*, 45 (6), 1945–1954, 2008.
[20] Ansari S.A., Knowles K. and Zbikowski R., Insectlike Flapping Wings in the Hover Part 2: Effect of Wing Geometry, *Journal of Aircraft*, 45 (6), 1976–1990, 2008.
[21] Rue J., Chang K., Ifju P., Haftka R.T., Schmitz T., McIntire J., Tyler C., Ganguly V., Chaudhuri A., Fabrication and Analysis of Small Flapping Wings, *Imaging Methods for Novel Materials and Challenging Applications*, Springer New York, 3, 337-344, 2013.
[22] Gogulapati A., Friedmann P.P. and Martins J.R.R.A., Optimization of the Kinematics of a Flapping wing MAV in Hover for Enhanced Performance, *54th AIAA/ASME/ASCE/AHS/ASC Structures, Structural Dynamics and Materials Conference*, Boston, MA, 8-11 April, 2013 (10.2514/6.2013-1646).
[23] Viana F.A.C., Haftka R.T., Hamman R. and Venter G., Efficient Global Optimization with Experimental Data: Revisiting the Paper Helicopter Design, *52nd AIAA/ASME/ASCE/AHS/ASC Structures, Structural Dynamics and Materials Conference*, Denver, Colorado, 4-7 April, 2011.
[24] Jones D., Schonlau M. and Welch W., Efficient global optimization of expensive black-box functions, *Journal of Global Optimization*, 13 (4), 455-492, 1998.
[25] Jones D.R., A taxonomy of global optimization methods based on response surfaces, *Journal of Global Optimization*, 21 (4), 345-383, 2001.
[26] Chaudhuri A., Haftka R.T., Viana F.A.C., Efficient Global optimization with adaptive target for Probability of target Improvement, *8th AIAA Multidisciplinary Design Optimization Specialist Conference*, Honolulu, USA, April 23-26, 2012.
[27] Viana F.A.C. and Haftka R.T., Surrogate-based optimization with parallel simulations using the probability of improvement, *13th AIAA/ISSMO Multidisciplinary Analysis and Optimization Conference*, Fort Worth, USA, September 13-15, 2010.
[28] Glüer C.-C., Blake G., Lu Y., Blunt B.A., Jergas M. and Genant H.K., Accurate assessment of precision errors: how to measure the reproducibility of bone densitometry techniques, *Osteoporosis* International, 5 (4), 262-270, 1995.
[29] Dransfield R.D. and Brightwell R., How to Get On Top of Statistics: Design & Analysis for Biologists, with R, *Influential Points LLP*, 2012.
[30] Trietsch Dan, Statistical Quality Control: A Loss Minimization Approach, World Scientific, pp. 170-173, 1999.
[31] Mckay M.D., Beckman R.J. and Conover W.J., A comparison of three methods for selecting values of input variables from a computer code, Technometrics, 21, 239-245, 1979.
[32] Viana F.A.C., Haftka R.T. and Steffen V. Jr, Multiple surrogates: how cross-validation errors can help us to obtain the best predictor, *Structural and Multidisciplinary Optimization*, 39 (4), 439-457, 2009.